

# The Reaction $\gamma\gamma \rightarrow \pi^0\pi^0$

## in Generalized Chiral Perturbation Theory

M. Knecht, B. Moussallam, J. Stern

*Division de Physique Théorique \*, Institut de Physique Nucléaire  
F-91406 Orsay Cedex, France*

### Abstract

The cross section for  $\gamma\gamma \rightarrow \pi^0\pi^0$  and the pion polarizabilities are computed, within generalized chiral perturbation theory, in the full one loop approximation, *i.e.* up to and including order  $O(p^5)$ . The result depends on the parameter  $\alpha_{\pi\pi}$  defining the tree level  $\pi - \pi$  scattering amplitude and on an additional low energy constant. The latter is shown to be related by an exact sum-rule to the  $e^+e^-$  data. The parameter  $\alpha_{\pi\pi}$  is related to the quark mass ratio  $r = m_s/\hat{m}$  via the expansion of pseudoscalar meson masses. The generalized one loop  $\gamma\gamma \rightarrow \pi^0\pi^0$  amplitude agrees with the experimental data in the threshold region provided  $r = m_s/\hat{m} \lesssim 10$ . Higher order corrections are estimated comparing our calculation with the dispersive approach.

IPNO/TH 94-08

January 1994

---

\*Unité de Recherche des Universités Paris XI et Paris VI associée au CNRS.

# 1 Introduction

The reaction  $\gamma\gamma \rightarrow \pi^0\pi^0$  at low energies provides a so far rare example of a probe of the chiral symmetry breaking sector of QCD for which experimental data already exist [1]. Moreover, these data do not exhibit any unexpected feature, as they can be reproduced without difficulty [2]-[7] using the standard methods based on dispersion relations, unitarity and resonance saturation. The one-loop prediction of the standard chiral perturbation theory [8] ( $\chi$ PT) appeared prior [9, 10] to the publication of the experimental results. It does not involve any free parameter and it disagrees with the data by several standard deviations even close to threshold. Recently, the full two-loop calculation has been completed by Bellucci, Gasser and Sainio [11]. It involves three new  $O(p^6)$  constants (estimated via resonance saturation) and it agrees with the experimental data within errors. The purpose of this work is to add one more information to this list: In the framework of *generalized*  $\chi$ PT (defined in [12, 13]), the agreement with experiment near threshold is already reached within the one-loop approximation, provided the ratio of quark masses  $r \equiv m_s/\hat{m}$  is considerably lower than usually expected, typically  $r \leq 10$ .

The important question to ask is: What can  $\gamma\gamma \rightarrow \pi^0\pi^0$  data tell us about the expansion of the QCD effective Lagrangian [14, 15]? While each individual term of  $\mathcal{L}^{eff}$  is uniquely determined [16] by symmetry properties of QCD, the relative importance of different terms depends on the actual values of the quark masses and of the low-energy constants characterizing the chiral structure of the QCD vacuum. The latter in turn determines how the expansion of  $\mathcal{L}^{eff}$  in powers of quark masses and external momenta should be organized such as to obtain a good convergence rate. The *standard chiral perturbation theory* [8] is an expansion which assumes that the quark masses  $m_u$ ,  $m_d$  and  $m_s$  are small enough not only with respect to the hadronic scale  $\Lambda_H \sim 1$  GeV, but also as compared to the scale  $B_0$  of the single flavour quark-antiquark condensate,  $\langle \bar{q}q \rangle_0 = -B_0 F_0^2$ , defined at  $m_u = m_d = m_s = 0$ . Within QCD, the last assumption is hard to justify *a priori*, since nothing prevents  $B_0$  to be as small as, say, the pion decay constant  $F_0 \sim 90$  MeV, *i.e.* much smaller than  $\Lambda_H$ . To illustrate the importance of the condition  $m_q \ll B_0$ , let us mention the fact that the standard relation between pseudoscalar meson and quark mass ratios [17] :

$$r = \frac{m_s}{\hat{m}} = 2 \frac{M_K^2}{M_\pi^2} - 1 + \dots = 25.9 + \dots, \quad \hat{m} \equiv \frac{1}{2}(m_u + m_d), \quad (1)$$

receives, at the next order, corrections [8, 18] (represented by the ellipses) which are of both types,  $O(m_q/\Lambda_H)$  and  $O(m_q/B_0)$ . On the other hand, the analysis of the Dashen-Weinstein sum-rule for the deviations from the Goldberger-Treiman relation suggests that  $r$  might differ considerably from the above value [19], *e.g.*  $r \leq 10$ . If confirmed<sup>1</sup>, this result could be interpreted as an experimental indication of an important  $O(m_q/B_0)$  contribution to Eq. (1).

---

<sup>1</sup>For a recent determination of the  $\pi N$  coupling constant, see Ref. [20]

The *generalized chiral perturbation theory* [12, 13] reformulates the expansion of the effective Lagrangian without assuming that  $m_q \ll B_0$ . It is as systematic and consistent as the standard  $\chi$ PT. At all orders in  $p/\Lambda_H$  and in  $m_q/\Lambda_H$ , both expansion schemes, standard and generalized, sum up the same effective Lagrangian  $\mathcal{L}^{eff.}$  of QCD. However, at each *finite* order, the generalized  $\chi$ PT takes into account terms which standard  $\chi$ PT relegates to higher orders. Already at the leading  $O(p^2)$  order, the generalized  $\chi$ PT involves more terms and more parameters: In particular, the quark mass ratio  $r$  is a free parameter, to be determined by experiment. In the limit  $r = r_2 \equiv 2M_K^2/M_\pi^2 - 1$ , one recovers the standard  $\chi$ PT as a special case. In practice, the generalized  $\chi$ PT is defined by the formal counting rule  $\hat{m}, m_s, B_0 \sim O(p)$  [12, 13], replacing the usual rule  $\hat{m}, m_s \sim O(p^2/\Lambda_H), B_0 \sim O(\Lambda_H)$  characteristic of standard  $\chi$ PT [8]. Hence, for  $p \ll \Lambda_H$ , one can write

$$\mathcal{L}^{eff.} = \mathcal{L}^{(2)} + \mathcal{L}^{(4)} + \mathcal{L}^{(6)} + \dots = \tilde{\mathcal{L}}^{(2)} + \tilde{\mathcal{L}}^{(3)} + \tilde{\mathcal{L}}^{(4)} + \tilde{\mathcal{L}}^{(5)} + \tilde{\mathcal{L}}^{(6)} + \dots, \quad (2)$$

where the first expansion is the standard one [8], whereas the second one corresponds to the generalized  $\chi$ PT.

In the next section, we summarize our results for the one-loop generalized  $\chi$ PT  $\gamma\gamma \rightarrow \pi^0\pi^0$  amplitude. It depends on the generalized tree-level  $\pi-\pi$  amplitude [12, 13] (kaon loops give only a small contribution) and it receives a constant shift from an order  $O(p^5)$  tree-level contribution. The latter is shown to be calculable, through a low-energy theorem, from  $e^+e^- \rightarrow$  hadrons data (Section 3). As an indicative estimate of higher order corrections, we submit, in Sect. 4, our result to a dispersive analysis along the lines of Ref. [4]. We finally add a few comments on charged and neutral pion polarizabilities.

We find it convenient to perform the whole analysis within the three-light-flavours  $\chi$ PT. It allows us to keep kaon loops under control and, mainly, it should help in establishing relationships to other observables (c.f. Sect. 3) and to similar processes such as  $\eta \rightarrow \pi^0\gamma\gamma$  [21].

## 2 $\gamma\gamma \rightarrow \pi^0\pi^0$ to generalized one loop order

In the present section, we establish the expression at generalized one loop order for the amplitude of the reaction  $\gamma\gamma \rightarrow \pi^0\pi^0$ . The modified chiral counting specific to generalized  $\chi$ PT leads to the appearance of terms of *odd* orders, which do not correspond to an increase in the number of loops, but to additional corrections in powers of the quark masses. Thus, the leading order contributions from  $\tilde{\mathcal{L}}^{(2)}$  receive tree-level corrections from  $\tilde{\mathcal{L}}^{(3)}$ , which come before the one loop effects. Similarly, before going to the two loop order, one has to take into account contributions at order  $O(p^5)$ . The generating functional (S-matrix) at one loop order in generalized  $\chi$ PT is thus given by the following expansion:

$$\mathcal{Z}^{eff.} = \tilde{\mathcal{Z}}_{tree}^{(2)} + \tilde{\mathcal{Z}}_{tree}^{(3)} + \tilde{\mathcal{Z}}_{tree}^{(4)} + \tilde{\mathcal{Z}}_{1loop}^{(4)} + \tilde{\mathcal{Z}}_{tree}^{(5)} + \tilde{\mathcal{Z}}_{1loop}^{(5)} + \dots. \quad (3)$$

Here,  $\tilde{\mathcal{Z}}_{tree}^{(2)}$  corresponds to all the tree diagrams made from an arbitrary number of vertices from  $\tilde{\mathcal{L}}^{(2)}$ ;  $\tilde{\mathcal{Z}}_{tree}^{(3)}$  denotes the same set of diagrams, but where a *single* vertex from  $\tilde{\mathcal{L}}^{(2)}$  is replaced by a vertex from  $\tilde{\mathcal{L}}^{(3)}$ .  $\tilde{\mathcal{Z}}_{tree}^{(4)}$  contains a single vertex from  $\tilde{\mathcal{L}}^{(4)}$  or *two* vertices from  $\tilde{\mathcal{L}}^{(3)}$ , with an arbitrary number of additional vertices from  $\tilde{\mathcal{L}}^{(2)}$ . Similarly,  $\tilde{\mathcal{Z}}_{tree}^{(5)}$  stands for all tree diagrams made from any number of vertices from  $\tilde{\mathcal{L}}^{(2)}$  and either a single vertex from  $\tilde{\mathcal{L}}^{(5)}$  or one vertex from  $\tilde{\mathcal{L}}^{(3)}$  and one vertex from  $\tilde{\mathcal{L}}^{(4)}$ . Finally,  $\tilde{\mathcal{Z}}_{1loop}^{(4)}$  stands for all one loop diagrams made with vertices from  $\tilde{\mathcal{L}}^{(2)}$  only, while  $\tilde{\mathcal{Z}}_{1loop}^{(5)}$  denotes the same diagrams, but with one of those vertices replaced by a vertex from  $\tilde{\mathcal{L}}^{(3)}$ .

The general analysis of  $\mathcal{Z}^{eff}$  up to and including the order  $O(p^5)$  (Eq. (3)) and of the various low-energy constants involved is beyond the scope of the present work, and will be given elsewhere [22]<sup>2</sup>. Here, we shall merely consider those terms which contribute to the matrix element

$$\langle \pi^0(p_1)\pi^0(p_2) out | \gamma(k_1, \epsilon_1)\gamma(k_2, \epsilon_2) in \rangle = ie^2(2\pi)^4 \delta^4(P_f - P_i) \epsilon_1^\mu \epsilon_2^\nu M_{\mu\nu} , \quad (4)$$

with<sup>3</sup>

$$M_{\mu\nu} = H(s, t, u) \left( \frac{s}{2} \eta_{\mu\nu} - k_{1\nu} k_{2\mu} \right) + \dots . \quad (5)$$

(The ellipses stand for the other Lorentz tensors in the general decomposition of  $M_{\mu\nu}$ , whose form factors receive contributions, for on-shell photons, only from order  $O(p^6)$  onward.) In this case, the terms  $\tilde{\mathcal{Z}}_{tree}^{(2)}$ ,  $\tilde{\mathcal{Z}}_{tree}^{(3)}$  and  $\tilde{\mathcal{Z}}_{tree}^{(4)}$  in Eq. (3) do not contribute. The remaining three terms contribute to the amplitude  $H(s, t, u)$ , the loop diagrams  $\tilde{\mathcal{Z}}_{1loop}^{(4)}$  and  $\tilde{\mathcal{Z}}_{1loop}^{(5)}$  and the tree diagrams of order  $O(p^5)$  are all separately finite. Topologically, the loop diagrams are the same as in the standard case [9], [10], but the vertices are to be read off from  $\tilde{\mathcal{L}}^{(2)}$  and from  $\tilde{\mathcal{L}}^{(3)}$ , where

$$\begin{aligned} \tilde{\mathcal{L}}^{(2)} &= \frac{F_0^2}{4} \left\{ \langle D^\mu U^+ D_\mu U \rangle + 2B_0 \langle \mathcal{M}_q (U + U^+) \rangle \right. \\ &+ A_0 \langle (\mathcal{M}_q U)^2 + (\mathcal{M}_q U^+)^2 \rangle \\ &\left. + Z_0^S \langle \mathcal{M}_q U + \mathcal{M}_q U^+ \rangle^2 + \dots \right\} , \end{aligned} \quad (6)$$

and

$$\begin{aligned} \tilde{\mathcal{L}}^{(3)} &= \frac{F_0^2}{4} \left\{ \xi \langle D^\mu U^+ D_\mu U (\mathcal{M}_q U + U^+ \mathcal{M}_q) \rangle \right. \\ &+ \tilde{\xi} \langle D^\mu U^+ D_\mu U \rangle \langle \mathcal{M}_q (U^+ + U) \rangle \\ &+ \rho_1 \langle (\mathcal{M}_q U)^3 + (\mathcal{M}_q U^+)^3 \rangle + \rho_2 \langle \mathcal{M}_q^3 (U + U^+) \rangle \\ &+ \rho_4 \langle (\mathcal{M}_q U)^2 + (\mathcal{M}_q U^+)^2 \rangle \langle \mathcal{M}_q (U + U^+) \rangle \\ &\left. + \rho_5 \langle \mathcal{M}_q^2 \rangle \langle \mathcal{M}_q (U + U^+) \rangle + \rho_7 \langle \mathcal{M}_q (U + U^+) \rangle^3 + \dots \right\} , \end{aligned} \quad (7)$$

<sup>2</sup>For a discussion of the leading order, see Ref. [12]

<sup>3</sup>The amplitude denoted by  $H(s, t, u)$  is called  $A(s, t, u)$  by the authors of Ref. [11]. We have adopted a different notation in order to avoid confusion with the standard notation  $A(s|t, u)$  for the  $\pi - \pi$  scattering amplitude.

with at most one vertex per diagram coming from  $\tilde{\mathcal{L}}^{(3)}$ . The notations are as given in Ref.[8],  $\mathcal{M}_q = \text{diag}(\hat{m}, \hat{m}, m_s)$  denotes the quark mass matrix and the ellipses stand for those terms which do not contribute to  $H(s, t, u)$ . The tree graph contributions of order  $O(p^5)$  are described by<sup>4</sup>

$$\begin{aligned} \tilde{\mathcal{L}}^{(5)} &= c_1 \langle F_L^{\mu\nu} \mathcal{M}_q F_{R\mu\nu} U + F_R^{\mu\nu} \mathcal{M}_q F_{L\mu\nu} U^+ \rangle \\ &+ c_2 \langle F_L^{\mu\nu} U^+ F_{R\mu\nu} U \mathcal{M}_q U + F_R^{\mu\nu} U F_{L\mu\nu} U^+ \mathcal{M}_q U^+ \rangle \\ &+ c_3 \langle F_R^{\mu\nu} F_{R\mu\nu} (U \mathcal{M}_q + \mathcal{M}_q U^+) + F_L^{\mu\nu} F_{L\mu\nu} (U^+ \mathcal{M}_q + \mathcal{M}_q U) \rangle \\ &+ c_4 \langle F_R^{\mu\nu} F_{R\mu\nu} + F_L^{\mu\nu} F_{L\mu\nu} \rangle \langle \mathcal{M}_q (U + U^+) \rangle + \dots \end{aligned} \quad (8)$$

The final result will only depend on  $F_\pi$ ,  $M_\pi$ , and on a few other independent combinations of  $\hat{m}$ , of  $r$ , and of the various low-energy constants occurring in (6), (7) and (8). The relevant vertices are given in Fig. 1. Up to the order  $O(p^5)$ , the amplitude  $H(s, t, u)$  depends only on  $s$ ,  $H(s, t, u) = H(s) + O(p^6)$ , and takes the following form

$$H(s) = A^{\pi\text{-loop}}(s) + A^{K\text{-loop}}(s) - \frac{4c}{F_\pi^2}. \quad (9)$$

The pion loop contribution  $A^{\pi\text{-loop}}$  may be written as

$$A^{\pi\text{-loop}}(s) = \frac{4}{s} \left[ \beta_{\pi\pi} \frac{s - \frac{4}{3}M_\pi^2}{F_\pi^2} + \alpha_{\pi\pi} \frac{M_\pi^2}{3F_\pi^2} \right] \bar{G}\left(\frac{s}{M_\pi^2}\right), \quad (10)$$

where  $\bar{G}$  denotes the following loop function,

$$-16\pi^2 \bar{G}(z) = \begin{cases} 1 + \frac{1}{z} (\ln \frac{1-\sigma}{1+\sigma} + i\pi)^2 & , \text{ if } 4 \leq z \\ 1 - \frac{4}{z} \text{arctg}^2\left(\frac{z}{4-z}\right)^{\frac{1}{2}} & , \text{ if } 0 \leq z \leq 4 \\ 1 + \frac{1}{z} \ln^2 \frac{\sigma-1}{\sigma+1} & , \text{ if } z \leq 0 \end{cases} \quad , \quad \sigma(z) \equiv \sqrt{1 - 4/z}. \quad (11)$$

Here  $\alpha_{\pi\pi}$  and  $\beta_{\pi\pi}$  are two combinations of the low-energy constants of  $\tilde{\mathcal{L}}^{(2)} + \tilde{\mathcal{L}}^{(3)}$  which parametrize the  $O(p^3)$  tree-level  $\pi - \pi$  scattering amplitude [12]

$$A(s | t, u) = \beta_{\pi\pi} \frac{s - \frac{4}{3}M_\pi^2}{F_\pi^2} + \alpha_{\pi\pi} \frac{M_\pi^2}{3F_\pi^2} + O(p^4). \quad (12)$$

The kaon loop contribution has a similar structure,

$$A^{K\text{-loop}}(s) = \frac{4}{s} \left[ \frac{\beta_{\pi K}}{4F_\pi^2} \left( s - \frac{2}{3}M_\pi^2 - \frac{2}{3}M_K^2 \right) + \frac{1}{6F_\pi^2} [(M_K - M_\pi)^2 + 2M_\pi M_K \alpha_{\pi K}] \right] \bar{G}\left(\frac{s}{M_K^2}\right), \quad (13)$$

---

<sup>4</sup>In standard  $\chi$ PT, these terms would be part of the  $O(p^6)$  contributions [11].

in terms of two other combinations of the low-energy constants,  $\alpha_{\pi K}$  and  $\beta_{\pi K}$ , which parametrize the  $O(p^3)$  tree-level  $K - \pi$  amplitude  $A^+(s, t, u)$  <sup>5</sup> [23], symmetric in  $s$  and  $u$ :

$$A^+(s, t, u) = \frac{\beta_{\pi K}}{4F_\pi^2} \left( t - \frac{2}{3}M_\pi^2 - \frac{2}{3}M_K^2 \right) + \frac{1}{6F_\pi^2} [(M_K - M_\pi)^2 + 2M_\pi M_K \alpha_{\pi K}] + O(p^4) . \quad (14)$$

It is useful to express  $\alpha_{\pi\pi}$  and  $\alpha_{\pi K}$  as

$$\begin{aligned} \alpha_{\pi\pi} &= \alpha_{\pi\pi}^{lead} + \delta\alpha_{\pi\pi} \\ \alpha_{\pi K} &= \alpha_{\pi K}^{lead} + \delta\alpha_{\pi K} , \end{aligned} \quad (15)$$

where  $\alpha_{\pi\pi}^{lead}$  and  $\alpha_{\pi K}^{lead}$  arise from  $\tilde{\mathcal{L}}^{(2)}$ , whereas  $\delta\alpha_{\pi\pi}$  and  $\delta\alpha_{\pi K}$  stem from  $\tilde{\mathcal{L}}^{(3)}$ . The explicit expressions for  $\delta\alpha_{\pi\pi}$  and for  $\delta\alpha_{\pi K}$  in terms of the low-energy constants appearing in  $\tilde{\mathcal{L}}^{(2)}$  and in  $\tilde{\mathcal{L}}^{(3)}$  will not be used in the sequel and can be obtained from the formulae collected in the Appendix. Similarly, one finds:

$$\beta_{\pi\pi} = 1 + 2\xi\hat{m} + 4\tilde{\xi}\hat{m} , \quad \beta_{\pi K} = 1 + 2\xi\hat{m} + 4\tilde{\xi}\hat{m}(3 + r) . \quad (16)$$

(In both cases, the leading order values are  $\beta_{\pi\pi}^{lead} = \beta_{\pi K}^{lead} = 1$ .) Finally, we come to the tree contribution from  $\tilde{\mathcal{L}}^{(5)}$  which gives a constant shift to  $H(s)$ , see (9), with

$$c = -\frac{10}{9}(c_1 + c_2 + 2c_3)\hat{m} - \frac{16}{3}c_4\hat{m} \approx -\frac{10}{9}(c_1 + c_2 + 2c_3)\hat{m} , \quad (17)$$

where the second, approximate, expression is obtained by invoking the Zweig rule. This constant shift in  $H(s)$  appears (along with other contributions) only at order  $O(p^6)$  in the standard approach and  $c$  is in fact related to the constant  $d_3$  of Ref. [11] (see the discussion at the end of Section 3). However, since the loop contributions to  $H(s)$  are finite by themselves,  $c$  is not renormalized at the order we are considering <sup>6</sup>. The value of  $c$  depends on  $r$  and will be discussed below.

First, let us consider the amplitude  $H(s)$  when contributions up to order  $O(p^4)$  alone are taken into account. In that case, the constants  $c$ ,  $\delta\alpha_{\pi\pi}$  and  $\delta\alpha_{\pi K}$  drop out, and only the leading,  $O(p^2)$ , expressions for the  $\pi - \pi$  and  $K - \pi$  amplitudes are involved. These essentially depend on  $F_\pi$ ,  $M_\pi$  and  $r$ , since [12], [13], [23],

$$\begin{aligned} \alpha_{\pi\pi}^{lead} &= 1 + 6 \frac{r_2 - r}{r^2 - 1} (1 + 2\zeta) \quad , \quad \beta_{\pi\pi}^{lead} = 1 \quad , \quad r_2 \equiv 2 \frac{M_K^2}{M_\pi^2} - 1 \sim 25.9 \quad , \\ \alpha_{\pi K}^{lead} &= 1 + \frac{r + 1}{r_1 + 1} (\alpha_{\pi\pi}^{lead} - 1) \quad , \quad \beta_{\pi K}^{lead} = 1 \quad , \quad r_1 \equiv 2 \frac{M_K}{M_\pi} - 1 \sim 6.3 \quad , \end{aligned} \quad (18)$$

<sup>5</sup>In terms of the  $K - \pi$  isospin amplitudes,  $A^+ = \frac{2}{3}A^{3/2} + \frac{1}{3}A^{1/2}$ .

<sup>6</sup>The fact that  $c$  is finite in our case, whereas the constant  $d_3$  of [11] is renormalized does not bear any contradiction, and will be explained later (Sect. 3).

and since the Zweig rule violating parameter  $\zeta \equiv Z_0^S/A_0$  is expected to be small. In fact, vacuum stability arguments impose the following bounds at leading order [13]:

$$r \geq r_1 , \quad (19)$$

and

$$0 \leq \zeta \leq \frac{1}{2} \frac{r - r_1}{r_2 - r} \cdot \frac{r + r_1 + 2}{r + 2} . \quad (20)$$

For  $r = r_2$ , one recovers the standard values of Weinberg [17]  $\alpha_{\pi\pi}^{lead} = \alpha_{\pi K}^{lead} = 1$ . For the critical value  $r = r_1$ , one obtains  $\alpha_{\pi\pi}^{lead} = \alpha_{\pi K}^{lead} = 4$  [12], [23], and for an intermediate value, say  $r \sim 10$ ,  $2 \leq \alpha_{\pi\pi}^{lead} \leq 2.3$ . Thus, as  $r$  decreases from its standard value  $r_2$  towards its critical value  $r_1$ ,  $\alpha_{\pi\pi}^{lead}$  varies by a factor four. This results in an increase of  $|H(s)|$  at order  $O(p^4)$  in the threshold region of about 25% when  $r$  ranges through the same values. The corresponding variation of the cross section is shown in Fig. 2.

At full one loop order, i.e. taking into account the order  $O(p^5)$  corrections, the amplitude  $H(s)$  no longer depends on  $r$  alone. It also involves the low-energy constants of  $\tilde{\mathcal{L}}^{(3)}$  and the combination (17) of low-energy constants from  $\tilde{\mathcal{L}}^{(5)}$ . We first notice that the constant  $\xi$  involved in the expressions (16) for  $\beta_{\pi\pi}$  and  $\beta_{\pi K}$  is also responsible for the splitting between  $F_\pi$  and  $F_K$  at order  $O(p^3)$  [12] (in the standard case, this splitting occurs only at order  $O(p^4)$ ):

$$F_\pi^2 = F_0^2 [1 + 2\hat{m}\xi + 2\hat{m}\tilde{\xi}(2 + r) + \dots] , \quad (21)$$

$$F_K^2 = F_0^2 [1 + \hat{m}\xi(1 + r) + 2\hat{m}\tilde{\xi}(2 + r) + \dots] . \quad (22)$$

Therefore,

$$\hat{m}\xi = \frac{1}{r - 1} \left( \frac{F_K^2}{F_\pi^2} - 1 \right) + \dots , \quad (23)$$

which allows us to express  $\beta_{\pi\pi}$  and  $\beta_{\pi K}$  in terms of  $r$ ,

$$\begin{aligned} \beta_{\pi\pi} &= 1 + \frac{2}{r - 1} \left( \frac{F_K^2}{F_\pi^2} - 1 \right) (1 + 2\tilde{\xi}/\xi) + \dots , \\ \beta_{\pi K} &= 1 + \frac{2}{r - 1} \left( \frac{F_K^2}{F_\pi^2} - 1 \right) [1 + 2(3 + r)\tilde{\xi}/\xi] + \dots , \end{aligned} \quad (24)$$

up to the ratio  $\tilde{\xi}/\xi$ , which is anyhow expected to be small, due to the Zweig rule. Notice that  $\xi$  and  $\tilde{\xi}$  are related to the low-energy constants  $L_5$  and  $L_4$  of Ref. [8], respectively. Up to higher order,  $O(p^6)$ , corrections we may further replace  $r$  in the above formulae by its expression  $r(\alpha_{\pi\pi})$  obtained from Eq. (18), but with  $\alpha_{\pi\pi}^{lead}$  replaced by  $\alpha_{\pi\pi} = \alpha_{\pi\pi}^{lead} + \delta\alpha_{\pi\pi}$  (we take  $F_K/F_\pi = 1.22$ ). Finally, we establish, in Sect. 3, the following sum-rule:

$$c = -\frac{5}{144\pi^2} \cdot \frac{1}{r - 1} \left\{ \int_{4M_\pi^2}^{\infty} \frac{ds}{s} [R_+(s) - 3R_-(s)] - \frac{1}{2} \ln \left( \frac{M_K}{M_\pi} \right) \right\} + O(m_q^2, m_q B_0) , \quad (25)$$

where  $R_+$  ( $R_-$ ) represents the cross section for  $e^+e^-$  into hadronic final states with even (odd) total G-parity, normalized to the cross section for  $e^+e^- \rightarrow \mu^+\mu^-$ . Again,  $r$  in the formula above is to be thought as expressed in terms of  $\alpha_{\pi\pi}$ . The evaluation of the integral in the narrow resonance approximation gives the following estimate:

$$c = -\frac{1}{r-1}(4.6 \pm 2.3) \times 10^{-3} . \quad (26)$$

Hence, up to the small contribution from the kaon loops, and up to the Zweig rule violations contained in  $\zeta$  and in  $\tilde{\xi}/\xi$ , we have been able to express the cross section for  $\gamma\gamma \rightarrow \pi^0\pi^0$  at order  $O(p^5)$  in terms of the single parameter  $\alpha_{\pi\pi}$ . This constant could, in principle, be extracted from  $\pi - \pi$  phase shifts, given sufficiently accurate data<sup>7</sup>. We recall that if standard  $\chi$ PT is correct, then  $\alpha_{\pi\pi}$  is close to 1. The smaller  $B_0$ , the more  $\alpha_{\pi\pi}$  increases towards  $\alpha_{\pi\pi} \sim 4$ . In Fig. 3, we show the cross section for the three values  $\alpha_{\pi\pi} = 1, 3$  and 4. For  $\alpha_{\pi\pi} \geq 3$ , our result agrees, within errors, with the data [1] in the threshold region. For  $\alpha_{\pi\pi} = 4$  (*i.e.* when the factor  $1/(r-1)$  in (24) and (25) is largest), we have checked that the cross section is indeed insensitive to the contribution coming from the kaon loops, by varying  $\alpha_{\pi K}$  in the range  $2 \leq \alpha_{\pi K} \leq 6$ , and by taking  $\beta_{\pi K}$  from Eq. (24). We have also checked that the result is insensitive to the variation of the constant  $c$  within the range  $-1.30 \times 10^{-3} \leq c \leq -0.44 \times 10^{-3}$  given by Eq. (26) for  $\alpha_{\pi\pi} = 4$ . Actually, even if we set  $c$  equal to zero, the low-energy cross section is only barely affected, see Fig. 4. On the other hand, the cross section is more sensitive to variations of  $\beta_{\pi\pi}$  coming from different values of the Zweig rule violating ratio  $\tilde{\xi}/\xi$ . Taking this ratio in the range  $-0.2 \leq \tilde{\xi}/\xi \leq +0.2$ , which amounts to a Zweig-rule violation of 40% in  $\beta_{\pi\pi}$  (and corresponds to the range allowed for  $L_4/L_5$  in [8]), we find the variations in the cross section as shown in Fig. 5.

### 3 A low-energy theorem for the $O(p^5)$ constant $c$

In this section, we derive the sum-rule (25) and discuss its numerical evaluation. Consider the decomposition of the electromagnetic current into its  $I=1$  and  $I=0$  components:

$$j_\mu = V_\mu^3 + \frac{1}{\sqrt{3}}V_\mu^8 , \quad (27)$$

where

$$V_\mu^3 = \frac{1}{2}(\bar{u}\gamma_\mu u - \bar{d}\gamma_\mu d) , \quad V_\mu^8 = \frac{1}{2\sqrt{3}}(\bar{u}\gamma_\mu u + \bar{d}\gamma_\mu d - 2\bar{s}\gamma_\mu s) . \quad (28)$$

The corresponding vacuum polarization functions,

$$i \int d^4x e^{iqx} \langle \Omega | T \{ V_\mu^a(x) V_\nu^a(0) \} | \Omega \rangle = (q_\mu q_\nu - \eta_{\mu\nu} q^2) \Pi^{aa}(q^2) , \quad a = 3, 8 , \quad (29)$$

---

<sup>7</sup>An analysis [13] of the available data shows that any value of  $\alpha_{\pi\pi}$  in a range  $\sim 1 - 4$  can be accounted for.



and

$$i \int d^4x e^{iq \cdot x} \langle \Omega | T \{ j_\mu^a(x) j_\nu^a(0) \} | \Omega \rangle = (q_\mu q_\nu - \eta_{\mu\nu} q^2) \Pi^{e.m.}(q^2), \quad (30)$$

satisfy

$$\Pi^{e.m.}(Q^2) = \Pi^{33}(q^2) + \frac{1}{3} \Pi^{88}(q^2), \quad (31)$$

if isospin violations due to the electromagnetic interactions and to  $m_u \neq m_d$  are neglected. Furthermore, the spectral density of the electromagnetic current is related to the inclusive  $e^+e^-$  cross section

$$\frac{1}{\pi} \Im m \Pi^{e.m.}(q^2) = \frac{1}{12\pi^2} R(q^2), \quad (32)$$

where, as usual,

$$R(q^2) = \frac{\sigma_{e^+e^- \rightarrow had.}(q^2)}{\sigma_{e^+e^- \rightarrow \mu^+\mu^-}(q^2)} = R_+(q^2) + R_-(q^2), \quad (33)$$

and where, corresponding to the decomposition (27),  $R(q^2)$  has been split into its contributions from G-parity even and from G-parity odd hadronic final states, with

$$\frac{1}{\pi} \Im m \Pi^{33}(q^2) = \frac{1}{12\pi^2} R_+(q^2), \quad \frac{1}{\pi} \Im m \Pi^{88}(q^2) = \frac{1}{4\pi^2} R_-(q^2). \quad (34)$$

The difference  $\Pi^{33}(q^2) - \Pi^{88}(q^2)$  then satisfies an unsubtracted dispersion relation, and consequently one can write the following sum-rule:

$$\Pi^{33}(0) - \Pi^{88}(0) = \frac{1}{\pi} \int_{4M_\pi^2}^{\infty} \frac{ds}{s} [\Im m \Pi^{33}(s) - \Im m \Pi^{88}(s)]. \quad (35)$$

On the other hand, the left-hand side of Eq. (35) above satisfies a low-energy theorem: From the generating functional  $\tilde{\mathcal{Z}}^{eff.}$  at order  $O(p^5)$ , one obtains:

$$\begin{aligned} \Pi^{33}(s) = & - 2[L_{10}^r(\mu) + 2H_1^r(\mu)] \\ & - 4(c_1 + c_2 + 2c_3)\hat{m} - 8c_4\hat{m}(2+r) \\ & + \frac{1}{3s}(s - 4M_\pi^2)\bar{J}\left(\frac{s}{M_\pi^2}\right) + \frac{1}{6s}(s - 4M_K^2)\bar{J}\left(\frac{s}{M_K^2}\right) \\ & - \frac{2}{3} \cdot \frac{1}{32\pi^2} \left( \ln \frac{M_\pi^2}{\mu^2} + 1 \right) - \frac{1}{3} \cdot \frac{1}{32\pi^2} \left( \ln \frac{M_K^2}{\mu^2} + 1 \right) + \frac{1}{48\pi^2} + O(s, \hat{m}^2, \hat{m}B_0), \end{aligned} \quad (36)$$

$$\begin{aligned} \Pi^{88}(s) = & - 2[L_{10}^r(\mu) + 2H_1^r(\mu)] \\ & - \frac{4}{3}(1 + 2r)(c_1 + c_2 + 2c_3)\hat{m} - 8c_4\hat{m}(2+r) \\ & + \frac{1}{2s}(s - 4M_K^2)\bar{J}\left(\frac{s}{M_K^2}\right) \\ & - \frac{1}{32\pi^2} \left( \ln \frac{M_K^2}{\mu^2} + 1 \right) + \frac{1}{48\pi^2} + O(s, \hat{m}^2, \hat{m}B_0). \end{aligned} \quad (37)$$

The low-energy constants  $L_{10}^r(\mu)$  and  $H_1^r(\mu)$  are as defined in [8]: they are common to both  $\mathcal{L}^{(4)}$  and  $\tilde{\mathcal{L}}^{(4)}$  since they are not associated with symmetry breaking terms,

$$L_{10}\langle U^+ F_{R\mu\nu} U F_L^{\mu\nu} \rangle + H_1\langle F_{R\mu\nu} F_R^{\mu\nu} + F_{L\mu\nu} F_L^{\mu\nu} \rangle \in \mathcal{L}^{(4)}, \tilde{\mathcal{L}}^{(4)}. \quad (38)$$

They depend on the renormalization scale  $\mu$ , again as specified in [8], but both  $\Pi^{33}$  and  $\Pi^{88}$  are independent of  $\mu$ . The loop function  $\bar{J}$  reads

$$\bar{J}(z) \equiv \frac{1}{16\pi^2} \left\{ \sigma \left( \ln \frac{1-\sigma}{1+\sigma} + i\pi \right) + 2 \right\}, \quad \sigma(z) \equiv \sqrt{1-4/z}, \quad (39)$$

for  $z \geq 4$ , and has the following expansion near  $z = 0$ ,

$$\bar{J}(z) = \frac{z}{96\pi^2} + O(z^2). \quad (40)$$

Taking the difference of Eqs. (36) and (37), and neglecting the Zweig rule violating constant  $c_4$  as in Eq. (17), one obtains the following sum-rule:

$$\begin{aligned} c &\sim -\frac{10}{9}(c_1 + c_2 + 2c_3)\hat{m} \\ &= -\frac{5}{12} \cdot \frac{1}{r-1} \left[ \frac{1}{\pi} \int_{4M_\pi^2}^{\infty} \frac{ds}{s} [\Im m\Pi^{33}(s) - \Im m\Pi^{88}(s)] - \frac{1}{24\pi^2} \ln\left(\frac{M_K}{M_\pi}\right) \right] + O(\hat{m}^2, \hat{m}B_0), \end{aligned} \quad (41)$$

which can now easily be written as given in Eq. (25). Notice also the presence of the overall factor  $1/(r-1)$  which suppresses the value of  $c$  when  $\alpha_{\pi\pi} \sim 1$ . The above sum-rule is similar to and should be compared with the sum-rule relating the scale invariant combination

$$\bar{L}_{10} \equiv L_{10}^r(\mu) + \frac{1}{144\pi^2} (\ln M_\pi^2/\mu^2 + 1) \quad (42)$$

to the difference of the spectral densities of the  $I = 1$  vector and axial currents [25].

The right-hand side of Eq. (41) expresses  $c$  as a difference of two contributions. The first one, represented by the dispersive integral, is numerically the most important one and positive, so that  $c$  comes out with a negative value. Writing this contribution as in Eq. (25) suggests a direct evaluation of the dispersive integral in terms of  $e^+e^-$  data. However, such data are not so easy to obtain, especially in the isoscalar channel, and are affected by large error bars. We refer to Ref. [26] for an overview of the experimental situation and for references. For our part, we shall evaluate the dispersive integral in the narrow resonance limit, taking into account contributions from  $\rho(768)$ ,  $\omega(782)$  and  $\phi(1020)$ :

$$\begin{aligned} \frac{1}{\pi} \int_{4M_\pi^2}^{\infty} \frac{ds}{s} [\Im m\Pi^{33}(s) - \Im m\Pi^{88}(s)]_{res.} &= \frac{3}{4\pi\alpha^2} \left\{ \frac{\Gamma_{\rho \rightarrow e^+e^-}}{M_\rho} - 3 \cdot \frac{\Gamma_{\omega \rightarrow e^+e^-}}{M_\omega} - 3 \cdot \frac{\Gamma_{\phi \rightarrow e^+e^-}}{M_\phi} \right\} \\ &\sim (11.1 \pm 2.0) \times 10^{-3}. \end{aligned} \quad (43)$$

The experimental values for the  $e^+e^-$  widths have been taken from the Particle Data Group compilation [27], and the error comes from the uncertainties on these numbers. The second term

on the right-hand side of Eq. (41) comes from contributions of virtual  $2\pi$  and  $2K$  intermediate states to the vacuum polarization functions  $\Pi^{33}(0)$  and  $\Pi^{88}(0)$ . Numerically, we have

$$\frac{1}{24\pi^2} \ln\left(\frac{M_K}{M_\pi}\right) = 5.4 \times 10^{-3} . \quad (44)$$

We estimate the contributions of non-resonant states to the dispersive integral by the size of this chiral logarithm. Indeed, if we evaluate the dispersive integral (43) replacing  $\Im m\Pi^{33}(s) - \Im m\Pi^{88}(s)$  by the imaginary parts as given by Eqs. (36) and (37), we precisely obtain this logarithm:

$$\frac{1}{\pi} \int_{4M_\pi^2}^{\infty} \frac{ds}{s} [\Im m\Pi^{33}(s) - \Im m\Pi^{88}(s)]_{\chi PT} = \frac{1}{24\pi^2} \ln\left(\frac{M_K}{M_\pi}\right) . \quad (45)$$

Hence, we do not add it to the contribution (43), but take it as our estimate of the uncertainty on the value of  $c$ , which we thus obtain as

$$c = -\frac{1}{r-1} \cdot (4.6 \pm 2.3) \times 10^{-3} . \quad (46)$$

For  $\alpha_{\pi\pi} = 4$ , one thus obtains  $c = -(0.87 \pm 0.43) \times 10^{-3}$ , whereas for  $\alpha_{\pi\pi} = 1$  this value comes out about five times smaller,  $c = -(0.18 \pm 0.09) \times 10^{-3}$ . This last value is relevant for the comparison with the constant  $d_3$  of Ref. [11]. At first sight, the fact that the latter is renormalized, whereas our  $O(p^5)$  constant is finite, might appear as puzzling. The point is that the divergent part of  $d_3$  comes with an additional power of  $B_0$ , and thus counts as order  $O(p^6)$  in generalized  $\chi$ PT. Therefore, the relationship between these two constants may be expressed as follows:

$$d_3^r(\mu) = -\frac{9F_\pi^2 c}{160\hat{m}B_0} \{1 + O(B_0 \ln \mu, \hat{m}) + \dots\} , \quad (47)$$

where the ellipses stand for additional corrections which might appear due to the fact that the constant  $c$  is defined in the three-light-flavours expansion scheme. In order to compare with the value of  $d_3^r$  extracted from standard  $\chi$ PT, in the numerical evaluation of Eq. (47) above one should take the value of  $c$  for  $\alpha_{\pi\pi} \approx 1$ , corresponding to the standard case, and consistently replace, up to higher orders,  $2\hat{m}B_0$  by  $M_\pi^2$ , *i.e.* consider  $B_0 \sim O(\Lambda_H)$ . This gives (notice that the sign is well defined)  $d_3^r(\mu) = (9.4 \pm 4.7) \times 10^{-6} + O(B_0 \ln \mu) + \dots$ , which is not incompatible with, say, the value of the scale invariant constant  $\bar{d}_3$  as computed from Appendix D of Ref. [11]:

$$\bar{d}_3 = \frac{F_\pi^2 C_S^\gamma C_S^m}{8M_S^2} \sim \pm 3.9 \times 10^{-6} . \quad (48)$$

It is possible to discuss the relationships between, say,  $\xi$  and  $L_5$ , or between  $\tilde{\xi}$  and  $L_4$ , along similar lines. This would, however, lead us too far astray, and we defer this discussion to forthcoming publications [28, 22].

## 4 Comparison with the dispersive approach

Morgan and Pennington [3] have devised a dispersion relation treatment of the  $\gamma\gamma \rightarrow \pi^0\pi^0$  amplitude which proved capable of representing the data quite correctly. The drawback of this type of approach is that the general principles of unitarity and analyticity do not completely constrain the amplitude. Donoghue and Holstein [4] argued that additional constraints should be provided by the chiral expansion. In this section, we discuss this idea, and we use the dispersive method, in conjunction with our  $O(p^5)$  results, as a means of estimating the size of higher order chiral corrections<sup>8</sup>.

In order to implement the method, one has to consider the charged channel  $\gamma\gamma \rightarrow \pi^+\pi^-$  as well as the neutral one. Let us designate by  $M_{\lambda\lambda'}^C$  and  $M_{\lambda\lambda'}^N$  the corresponding helicity amplitudes, normalized as in Eq. (3), and introduce the J=0 projections:

$$f_C(s) = \frac{1}{8\pi} \int d\Omega M_{++}^C, \quad f_N(s) = \frac{1}{8\pi} \int d\Omega M_{++}^N, \quad (49)$$

where  $f_N(s)$  is related to the amplitude defined in Eqs. (4), (5),  $H(s, t, u) = H(s) + O(p^6)$ , by  $H(s) = 4f_N(s)/s$ . Next, one introduces isospin combinations  $f_I(s)$ ,  $I = 0, 2$  [3] [4] which diagonalize the elastic unitarity relation:

$$f_C = \frac{2}{3}f_0 + \frac{1}{3}f_2, \quad f_N = \frac{2}{3}(f_0 - f_2). \quad (50)$$

Below the  $K\bar{K}$  threshold, the following representation holds for these functions [3]:

$$f_I(s) = l_I(s) + \Omega_I(s)s \left\{ \gamma_I + (s_0 - s) \frac{1}{\pi} \int_{4M_\pi^2}^{\infty} \frac{dx}{x} \frac{l_I(x) \Im m(1/\Omega_I(x))}{(x - s_0)(x - s - i\epsilon)} \right\}, \quad (51)$$

where  $\Omega_I(s)$  is the Omnès-Mushkelishvili [29] function constructed from the  $\pi - \pi$  phase shifts  $\delta_I(s)$  in the isospin channel  $I$ ,

$$\Omega_I(s) = \exp \left[ \frac{s}{\pi} \int_{4M_\pi^2}^{\infty} \frac{dx}{x} \frac{\delta_I(x)}{(x - s - i\epsilon)} \right], \quad (52)$$

(normalized such that  $\Omega_I(0) = 1$ ) and  $s_0$  is an arbitrary subtraction point. The function  $l_I(s)$  must have the same left-hand cut structure as the amplitude  $f_I(s)$  and be analytic in the rest of the complex  $s$  plane. The representation (51) then guarantees that  $f_I(s)$  has the correct analytic structure. In particular, the discontinuity along the right-hand cut  $4M_\pi^2 < s < \infty$  is given by:

$$\Im m f_I(s) = f_I(s) e^{-i\delta_I(s)} \sin \delta_I(s). \quad (53)$$

In the left-hand cut function one can separate the single pion pole (Born term)

$$l_I(s) = \frac{4M_\pi^2}{s\sigma(s/M_\pi^2)} \operatorname{arctanh} \sigma\left(\frac{s}{M_\pi^2}\right) + \tilde{l}_I(s). \quad (54)$$

---

<sup>8</sup>We are indebted to J. Gasser for repeatedly emphasizing this point to us.

The remaining piece,  $\tilde{l}_I(s)$ , is generated by two or more pion exchanges in the t (u) channels and shows up in the chiral expansion starting at order  $O(p^6)$ . A factor of  $s$  has been separated in Eqs. (51) and (54) on account of low-energy electromagnetic theorems and a single arbitrary constant (in each isospin channel) appears due to boundedness properties for asymptotic values of  $s$ .

It should be clear that a rigorous evaluation of the left-hand cut function  $\tilde{l}_I(s)$  is no simple matter. In fact, this can be done only order by order in chiral perturbation theory. For the purpose of doing order of magnitude estimates, however, it seems reasonable to retain the contributions of a few low-lying resonances:  $\rho$ ,  $\omega$ ,  $a_1$  and  $b_1$  [30]. The low energy region of interest here,  $2M_\pi \leq E_{\pi\pi} \leq 450$  MeV proves to be fairly insensitive to the details of which resonances are included and how they are parametrized [3]. This leaves one with the task of determining the arbitrary constants  $\gamma_I$ . Following the suggestion of [4], one should be able to do so by matching the dispersive representation (51) with the  $\chi$ PT prediction,  $f_I^\chi(s)$ , in a point where the latter can be trusted. It is of course convenient to choose the subtraction point in (51) equal to the matching point, so that the constants  $\gamma_I$  are simply given by:

$$\gamma_I = \frac{f_I^\chi(s_0) - l_I(s_0)}{s_0 \Omega_I(s_0)}. \quad (55)$$

One has then to extend the  $\chi$ PT calculation to the charged channel and one finds, for the isospin functions  $f_I^\chi(s)$ :

$$f_I^\chi(s) = \frac{4M_\pi^2}{s\sigma(s/M_\pi^2)} \operatorname{arctanh} \sigma\left(\frac{s}{M_\pi^2}\right) + A_I^\pi(s) \bar{G}\left(\frac{s}{M_\pi^2}\right) + A_I^K(s) \bar{G}\left(\frac{s}{M_K^2}\right) + \frac{2(L_9 + L_{10})s}{F_\pi^2} - \frac{\Delta_I s}{F_\pi^2} \quad (56)$$

where

$$A_0^\pi = \frac{1}{6F_\pi^2} [M_\pi^2(5\alpha_{\pi\pi} - 8\beta_{\pi\pi}) + 6\beta_{\pi\pi}s], \quad A_2^\pi = \frac{1}{6F_\pi^2} [M_\pi^2(2\alpha_{\pi\pi} + 4\beta_{\pi\pi}) - 3\beta_{\pi\pi}s], \quad (57)$$

$$A_0^K = \frac{1}{4F_\pi^2} \left[ \beta_{\pi K} \left( \frac{3}{2}s - M_\pi^2 - M_K^2 \right) + 2\alpha_{\pi K} M_\pi M_K + (M_K - M_\pi)^2 \right], \quad A_2^K = 0, \quad (58)$$

and where the function  $\bar{G}$  was defined in Eq. (11).  $f_I^\chi$  contains a contribution of order  $O(p^2) + O(p^3) + O(p^4)$  as well as a set of contributions of chiral order five which are collected in the constants  $\Delta_I$ . The combination  $c = 2(\Delta_0 - \Delta_2)/3$  was evaluated in Sec. 3. In contrast, we do not know of a simple way to estimate the combination  $c_+ = (2\Delta_0 + \Delta_1)/3$  which contributes to the  $\pi^+\pi^-$  channel. In principle, of course,  $\Delta_I$  can be evaluated from experiment via  $\chi$ PT analysis of the reactions  $\pi \rightarrow e\nu\gamma$ ,  $K \rightarrow e\nu\gamma$  and of the mean charge radii of the pion and the of kaon. One expects the size of  $c_+$  to be of order 10-30% that of  $L_9 + L_{10}$ , so that it can be absorbed to some extent into the uncertainty in the numerical value of  $L_9 + L_{10}$  (note that for consistency this numerical value itself should be determined here from an  $O(p^5)$  analysis).

We have included the contribution of the kaon loop in (56) for completeness, but since the corresponding  $K\bar{K}$  discontinuity is not accounted for in the dispersive formula (this could in principle be done following Ref. [31]), we do not include it when we perform the matching. It is worth noting that the chiral formula (56) satisfies the general dispersive representation: at this order, one has to set  $\tilde{l}_I(s) = 0$ ,  $\Omega_I(s) = 1$  and  $\Im m(1/\Omega_I(x)) = -\sigma(s/M_\pi^2)A_I^\pi(s)/16\pi$  in Eq. (51).

One should be aware that there are some ambiguities in the dispersive approach. Consider first the question of the matching point  $s_0$  in (55). The authors of Ref. [4], for instance, have matched the  $O(p^4)$   $\chi$ PT amplitude with a dispersive representation not including the vector meson contributions at  $s = 0$ . A priori, one would expect that any point in the region  $0 \leq s_0 \leq 4M_\pi^2$ , where the amplitude is real, should be as good as another. In practice though, the results are sensitive to which point is chosen. We will show the results corresponding to the two extreme cases  $s_0 = 0$  and  $s_0 = 4M_\pi^2$ . A further source of uncertainty, in the dispersive approach, comes from the  $\pi - \pi$  phase-shifts themselves. Clearly, what will matter most in the calculation is how the phase-shifts behave close to threshold. This threshold behaviour is usually parametrized in terms of the scattering lengths and of the slope parameters. Experimentally though, the phase-shifts have been extracted only for energies larger than 600 MeV. Extrapolation down to the threshold, even upon using constraints from the Roy equations and from  $Kl_4$  data, is subject to some uncertainty. The influence of this uncertainty on the  $\gamma\gamma \rightarrow \pi^0\pi^0$  dispersive amplitude has been considered in ref. [3]. Furthermore, in our case, the matching requires that one knows the relation between the constants  $\alpha_{\pi\pi}$ ,  $\beta_{\pi\pi}$  and the set of phase-shifts. This relationship has been studied in Ref. [13] and we will rely on its results in what follows. Consider the simple parametrization proposed by Schenk [32]:

$$\tan \delta_I(s) = \sqrt{1 - \frac{4M_\pi^2}{s}} \left[ a_I + \tilde{b}_I \left( \frac{s}{4M_\pi^2} - 1 \right) + c_I \left( \frac{s}{4M_\pi^2} - 1 \right)^2 \right] \left( \frac{4M_\pi^2 - E_I^2}{s - E_I^2} \right), \quad (59)$$

where  $\tilde{b}_I$  is related to the slope parameter  $b_I$  by  $\tilde{b}_I = b_I - a_I 4M_\pi^2 / (E_I^2 - 4M_\pi^2) + (a_I)^3$ . For  $I = 0$  we take two sets of parameters resulting from two fits to the production data obtained by fixing the value of the scattering length to  $a_0 = 0.26$ :

$$a) \ a_0 = 0.26, \ b_0 = 0.203, \ c_0 = -0.0126, \ E_0 = 813.3\text{MeV} \quad (60)$$

$$b) \ a_0 = 0.26, \ b_0 = 0.324, \ c_0 = -0.0274, \ E_0 = 863.1\text{MeV}, \quad (61)$$

which correspond to the data of Eastabrooks-Martin [33] and of Ochs [34], respectively. The two sets differ essentially by the value of the slope parameter  $b_0$ . The corresponding values of our low-energy parameters are [13]:

$$a) \ \alpha_{\pi\pi} = 3.35 \quad b) \ \alpha_{\pi\pi} = 4.10, \quad (62)$$

respectively, while  $\beta_{\pi\pi} = 1.17$  in both cases. The isospin  $I = 2$  parameters are taken as in Ref. [32]. Given a matching point  $s_0$ , we now have all the ingredients needed for a determination of the constants  $\gamma_I$  via (55) and the evaluation of the dispersive amplitudes from (51).

In Figs. 6a and 6b we compare the dispersive evaluation of the amplitude  $H(s)$  (or more precisely  $100M_\pi^2 H(s)$  for  $0 \leq s \leq 4M_\pi^2$  and  $100M_\pi^2 |H(s)|$  above threshold) for  $\gamma\gamma \rightarrow \pi^0\pi^0$ , corresponding to the two parameter sets (60) and (61) of  $\pi - \pi$  phases to our  $O(p^5)$  chiral calculation. The experimental points correspond to the Crystal Ball data [1] under the assumption that only the S-wave contributes to the cross section. One observes that in the case of the phases determined from (60) (Fig. 6a) the two dispersive representations (corresponding to  $s_0 = 0$  and  $s_0 = 4M_\pi^2$ ), the chiral calculation, as well as the experimental data are all rather close to each other in all the physical low-energy region of interest. On the contrary, in the case of the parameters (61) the dispersive amplitude always exceeds both the experimental data and the perturbative amplitude. This is presumably due to the fact that this set of phases is characterized by a slope parameter which is too large (the scattering length being chosen to be  $a_0 = 0.26$  in both cases). We note that the  $\gamma\gamma \rightarrow \pi^0\pi^0$  data provide only indirect information on the low energy behaviour of the  $\pi - \pi$  phases. On the other hand, the chiral representation allows to constrain the low energy parameters  $\alpha_{\pi\pi}$  and  $\beta_{\pi\pi}$ , which are related in a non-trivial way to the phases [13]. One further observes that the difference between the two dispersive curves with matching at 0 and  $4M_\pi^2$ , respectively, is most significant around  $s = 0$ . The amplitude is rather small in this region and corrections appear to be large. For instance the  $O(p^6)$  contribution coming from the vector mesons is about 50% of the  $O(p^5)$  chiral amplitude at  $s = 0$ , while it represents a negligible 5% at threshold.

Finally, we turn to the question of the pion polarizabilities. Due to our lack of knowledge of the  $O(p^5)$  corrections  $\Delta_I$  (see Eq. (56)) the charged pion polarizabilities can only be given to generalized  $O(p^4)$  order:

$$\bar{\alpha}_{\pi^+} = \frac{\alpha}{M_\pi F_\pi^2} \left[ \frac{1}{144\pi^2} (\alpha_{\pi\pi} - \beta_{\pi\pi}) + \frac{1}{576\pi^2} \lambda_K + 4(L_9 + L_{10}) + O(p^5) \right], \quad (63)$$

where

$$\lambda_K = 2(\alpha_{\pi K} - 1) \frac{M_\pi}{M_K} + (1 - \beta_{\pi K}) \left( 1 + \frac{M_\pi^2}{M_K^2} \right). \quad (64)$$

For the neutral pion, we find

$$\bar{\alpha}_{\pi^0} = \frac{\alpha}{M_\pi F_\pi^2} \left[ \frac{1}{288\pi^2} (\alpha_{\pi\pi} - 4\beta_{\pi\pi}) + \frac{1}{576\pi^2} \lambda_K - 2c \right]. \quad (65)$$

The difference with the standard  $O(p^4)$  situation is that, firstly,  $\alpha_{\pi\pi}$  and  $\beta_{\pi\pi}$  (as well as  $\alpha_{\pi K}$  and  $\beta_{\pi K}$ ) can depart significantly from the value 1 (the values used in the table below are those quoted in (62)). Secondly, we have extra contributions which are of chiral order five. In order to get a feeling of how significant these differences are, we have collected a few numerical values in Table (1) below:

	$\bar{\alpha}_{\pi^0}$	$\bar{\beta}_{\pi^0}$	$\bar{\alpha}_{\pi^+}$	$\bar{\beta}_{\pi^+}$
standard $O(p^4)$	-0.50	0.50	2.74	-2.74
standard $O(p^6)$ [11]	-0.35	1.50		
generalized $O(p^5)$	0.44	-0.44	3.47	-3.47
dispersive( $s_0 = 4M_\pi^2$ )	-0.76	1.78	3.33	-3.05
dispersive( $s_0 = 0$ )	0.96	0.07	3.61	-3.33

**Table 1:** Results for the electric ( $\bar{\alpha}$ ) and magnetic ( $\bar{\beta}$ ) pion polarizabilities in units of  $10^{-4} \text{ fm}^3$ .

The dispersive results are evaluated using the phase-shift parameters (60), and the values of  $\alpha_{\pi\pi}$ ,  $\beta_{\pi\pi}$  used in the  $O(p^5)$  expressions (63-65) correspond to the same phases (see (62a)). We proceed as follows. First, the difference in the electric and magnetic polarizations are obtained from

$$\bar{\alpha}_{\pi^0} - \bar{\beta}_{\pi^0} = \frac{\alpha}{M_\pi} \lim_{s=0} \frac{4f_N(s)}{s}, \quad (66)$$

( $f_N$  being calculated from the representation (51)) and similarly for the  $\pi^+$  with  $f_N$  replaced by  $f_C$ . Next, we assume that the polarization sum is saturated by the spin one meson pole contributions (the conventions and notations follow Ref. [11]):

$$\bar{\alpha}_{\pi^0} + \bar{\beta}_{\pi^0} = \frac{\alpha}{M_\pi} 8M_\pi^2 \left( \frac{C_\rho}{M_\rho^2 - M_\pi^2} + \frac{C_\omega}{M_\omega^2 - M_\pi^2} + \frac{C_{b_1}}{M_{b_1}^2 - M_\pi^2} \right), \quad (67)$$

with  $C_\omega = 0.67$ ,  $C_\rho = 0.12$ ,  $C_{b_1} = 0.53$  (all in  $\text{GeV}^{-2}$ ) for the  $\pi^0$ , while for the charged pion the sum is given by the same formula with  $C_\omega = 0$ ,  $C_\rho = 0.06$ , and  $C_{b_1}$  as before. These values are obtained from the experimental rates  $V^0 \rightarrow \pi^0\gamma$  and  $V^+ \rightarrow \pi^+\gamma$  respectively. Note the strong breaking of isospin symmetry for the  $\rho$  which is due to  $\rho - \omega$  mixing.

The table shows that the difference between the standard and the generalized  $\chi$ PT is rather minor for the charged pion which, in both cases, is dominated by  $L_9 + L_{10}$ . Things are quite different for the neutral pion since, in this case, we find the electric polarizability to be positive. This result is essentially caused by the  $O(p^5)$  constant  $c$  in formula (65). This contribution is much larger than the corresponding one in the  $O(p^6)$  calculation of Ref. [11] because of the  $1/(r-1)$  factor in (26) which is much larger in our case. It is also striking that the dispersive results with different matching points to the  $\chi$ PT amplitude yield rather different numbers for the polarizations. Note finally that the kaon loop contribution, which one would a priori expect to be negligible (and which is not included in the numbers shown in the table) would further increase the generalized  $O(p^5)$  value of  $\bar{\alpha}_{\pi^0}$  by 20%. This suggests that the neutral pion polarizabilities may be as difficult to control theoretically as they are difficult to measure experimentally.



## 5 Summary and concluding remarks

**i)** At the one loop order of generalized  $\chi$ PT, the  $\gamma\gamma \rightarrow \pi^0\pi^0$  amplitude consists of three parts which are all separately finite: The one loop  $O(p^4)$  and  $O(p^5)$  parts, and the tree level  $O(p^5)$  contribution, the latter representing a constant shift in the amplitude  $H(s)$ . Neglecting kaon loops and Zweig rule violating effects (described in standard  $\chi$ PT by the constants  $L_4$  and  $L_6$ ), the whole amplitude can be expressed in terms of the parameter  $\alpha_{\pi\pi}$  and of the single constant  $c$  describing the tree contribution of  $\tilde{\mathcal{L}}^{(5)}$ . We have derived a low-energy theorem which relates the constant  $c$  to the experimental cross section for  $e^+e^- \rightarrow \text{hadrons}$  and to  $\alpha_{\pi\pi}$ .

**ii)** The constant  $\alpha_{\pi\pi}$  is measurable in the low-energy  $\pi - \pi$  scattering [13]. Its leading  $O(p^2)$  part  $\alpha_{\pi\pi}^{lead}$  is a function of the quark mass ratio  $r = m_s/\hat{m}$ . Within the standard  $\chi$ PT,  $\alpha_{\pi\pi}$  should remain close to  $\alpha_{\pi\pi}^{lead} = 1$  ( $r \sim r_2 = 25.9$ ). The generalized  $\chi$ PT admits a substantially larger value of  $\alpha_{\pi\pi}$ , typically  $\alpha_{\pi\pi} \approx \alpha_{\pi\pi}^{lead} \lesssim 4$ , corresponding to  $r \gtrsim r_1 = 6.3$ . For energies  $E_{\pi\pi} < 450$  MeV, the generalized one loop cross section agrees with the Crystal Ball data [1] within errors, provided that  $\alpha_{\pi\pi} \geq 3$  (implying  $r < 10$ ). The low-energy cross section is barely affected by the uncertainties in the determination of the constant  $c$ .

**iii)** At order  $O(p^5)$  of generalized  $\chi$ PT, the neutral pion polarizability  $(\bar{\alpha} - \bar{\beta})_{\pi_0}$  becomes positive, typically  $(\bar{\alpha} - \bar{\beta})_{\pi_0} = (1.04 \pm 0.60) \times 10^{-4} \text{fm}^3$  for  $\alpha_{\pi\pi} = 3$ . This has to be compared with the values  $-1 \times 10^{-4} \text{fm}^3$  and  $-1.85 \times 10^{-4} \text{fm}^3$  predicted by the *standard*  $O(p^4)$  and  $O(p^6)$  orders [11], respectively. ( $\bar{\alpha} + \bar{\beta} = 0$  up to and including order  $O(p^5)$ .) This result is due to the fact that in generalized  $\chi$ PT the negative  $O(p^4)$  contribution is strongly suppressed due to the proximity of the Adler zero, which for  $\alpha_{\pi\pi}^{lead} \rightarrow 4$  moves towards the point  $s = 0$ . The polarizability is then dominated by the positive  $O(p^5)$  tree contribution. On the other hand, our prediction for the charged pion polarizabilities (Table 1) does not differ very much from the standard  $O(p^4)$  result. Notice that in this case, we have no quantitative control of the  $O(p^5)$  constant contribution.

**iv)** To illustrate the convergence rate of the generalized  $\chi$ PT, one may first compare the  $O(p^4)$  and  $O(p^5)$  contributions to the amplitude  $H(s)$ . For  $\alpha_{\pi\pi} = 3$ , the value of  $H(s)$  (multiplied by  $100M_\pi^2$ ) at threshold is 8.64, of which 7.23 come from  $O(p^4)$  loops, 0.81 from  $O(p^5)$  loops and the remaining 0.60 represent the  $O(p^5)$  tree contribution. Next, in order to control whether, at sufficiently low energies, the one loop generalized  $\chi$ PT correctly accounts for rescattering effects and final state interactions, we have compared our  $O(p^5)$  perturbative amplitude with a dispersion-theoretic amplitude which satisfies exact S-wave unitarity. For  $\alpha_{\pi\pi} \geq 3$  and for  $\pi - \pi$  phase-shifts not characterized by a too large slope parameter, we have found that the dispersive and perturbative amplitudes do indeed agree reasonably well for  $E_{\pi\pi} < 450$  MeV, and that there is no conflict with unitarity in this energy range. These facts

enforce the hope that higher orders of generalized  $\chi$ PT will remain sufficiently small, such as not to spoil the agreement with experiment.

It might be legitimate to ask that, at sufficiently low energies,  $\chi$ PT should correctly reproduce experimental data without resorting to higher orders, unless it is justified by kinematical reasons or by the high precision of the data. In the case of the reaction  $\gamma\gamma \rightarrow \pi^0\pi^0$ , the standard expansion of  $\mathcal{L}^{eff}$  fails to satisfy this requirement. The present analysis suggests a possible interpretation of this fact: At each order, the standard  $\chi$ PT misses important *symmetry breaking* terms which are unduly relegated to higher orders. In order to recover these terms and to reach agreement with experiment, one then has to go up to unnaturally high orders of  $\chi$ PT. If this conjecture turned out to be correct, similar phenomena could be expected elsewhere (low-energy  $\pi - \pi$  scattering, pion scalar form factors, symmetry breaking aspects of  $K_{l4}$  decays, etc.). In order to decide whether the generalized  $\chi$ PT provides a relevant improvement of the standard expansion of  $\mathcal{L}^{eff}$ , and whether the values of the various low-energy parameters ( $B_0$ ,  $r = m_s/\hat{m}, \dots$ ) should be revised correspondingly, additional experimental informations are needed. More precise data on low-energy  $\gamma\gamma \rightarrow \pi^0\pi^0$  and on the related process  $\eta \rightarrow \pi^0\gamma\gamma$  will be welcome. Decisive information might come from the model independent determination of low-energy  $\pi - \pi$  phase shifts and of  $K_{l4}$  form factors at DaΦne, as well as from a direct measurement of light quark masses in exclusive tau decays [35].

## Acknowledgements

We thank Jürg Gasser and Mikko Sainio for useful discussions.

## Appendix

We have gathered, in this Appendix, a few formulae related to the discussion in Section 2. The explicit expressions of the combinations  $M_\pi^2\alpha_{\pi\pi}$  and  $(M_K - M_\pi)^2 + 2M_\pi M_K\alpha_{\pi K}$  in terms of the low-energy constants of  $\tilde{\mathcal{L}}^{(2)}$  and of  $\tilde{\mathcal{L}}^{(3)}$  read as follows:

$$\begin{aligned}
M_\pi^2\alpha_{\pi\pi} &= 2\hat{m}B_0 + 4\hat{m}^2(4A_0 + 8Z_0^S + rZ_\pi^S) \\
&- 4\hat{m}^2B_0[3\xi + \tilde{\xi}(6 + r)] \\
&- 16\hat{m}^3A_0[3\xi + 2\tilde{\xi}(3 + r)] \\
&- 8\hat{m}^3Z_0^S[3\xi(4 + r) + \tilde{\xi}(24 + 14r + r^2)] \\
&+ \hat{m}^3[81\rho_1 + \rho_2 + 2\rho_4(82 + 16r + r^2) + \rho_5(2 + r^2) + 12\rho_7(2 + r)(14 + r)] ,
\end{aligned}$$

and

$$\begin{aligned}
(M_K - M_\pi)^2 &+ 2M_\pi M_K \alpha_{\pi K} = \\
&= \hat{m} B_0 (3 + r) + \hat{m}^2 A_0 (17 + 14r + r^2) + 2\hat{m}^2 Z_0^S (18 + 17r + r^2) \\
&- \hat{m}^2 B_0 [\xi(1 + r)(11 + r) + 2\tilde{\xi}(12 + 17r - r^2)] \\
&- \hat{m}^3 A_0 [\xi(1 + r)(29 + 18r + r^2) + 2\tilde{\xi}(40 + 71r + 18r^2 - r^3)] \\
&- \hat{m}^3 Z_0^S [(1 + r)(68 + 50r + 2r^2) + 2\tilde{\xi}(2 + r)(64 + 42r - 2r^2)] \\
&+ 2\hat{m}^3 \left[ \frac{3}{4}\rho_1(43 + 50r + 14r^2 + r^3) \right. \\
&\quad \left. + \frac{1}{4}\rho_2(3 + r^2) \right. \\
&\quad \left. + \frac{1}{2}\rho_4(146 + 188r + 59r^2 + 3r^3) \right. \\
&\quad \left. + \frac{1}{4}\rho_5(2 + r^2)(3 + r) \right. \\
&\quad \left. + 3\rho_7(2 + r)(30 + 29r + r^2) \right].
\end{aligned}$$

The order  $O(p^3)$  expressions for the pseudoscalar masses are given as:

$$\begin{aligned}
M_\pi^2 &= 2\hat{m} B_0 + 4\hat{m}^2 A_0 + 4\hat{m}^2 Z_0^S (2 + r) \\
&- 4\hat{m}^2 B_0 [\xi + \tilde{\xi}(2 + r)] \\
&- 8\hat{m}^3 A_0 [\xi + \tilde{\xi}(2 + r)] \\
&- 8\hat{m}^3 (2 + r) Z_0^S [\xi + \tilde{\xi}(2 + r)] \\
&+ \hat{m}^3 \left[ 9\rho_1 + \rho_2 \right. \\
&\quad \left. + 2\rho_4(10 + 4r + 4r^2) + \rho_5(2 + r^2) \right. \\
&\quad \left. + 12\rho_7(2 + r)^2 \right],
\end{aligned}$$

and

$$\begin{aligned}
M_K^2 &= \hat{m} B_0 (1 + r) + \hat{m}^2 A_0 (1 + r)^2 + 2\hat{m}^2 Z_0^S (2 + r)(1 + r) \\
&- \hat{m}^2 (1 + r) B_0 [\xi(1 + r) + 2\tilde{\xi}(2 + r)] \\
&- \hat{m}^3 (1 + r)^2 A_0 [\xi(1 + r) + 2\tilde{\xi}(2 + r)] \\
&- 2\hat{m}^3 (1 + r)(2 + r) Z_0^S [\xi(1 + r) + 2\tilde{\xi}(2 + r)] \\
&+ \hat{m}^3 (1 + r) \left[ \frac{3}{2}\rho_1(1 + r + r^2) + \frac{1}{2}\rho_2(1 - r + r^2) \right. \\
&\quad \left. + 3\rho_4(2 + 2r + r^2) + \frac{1}{2}\rho_5(1 + r + r^2) \right. \\
&\quad \left. + 6\rho_7(2 + r)^2 \right].
\end{aligned}$$

Combining these formulae, one may obtain the expressions for  $\alpha_{\pi\pi}$  and of  $\alpha_{\pi K}$ . At leading order, *i.e.* when  $\xi, \tilde{\xi}, \rho_1, \dots, \rho_7$  are set equal to zero, one can express  $\hat{m} B_0$  and  $\hat{m}^2 A_0$  in terms of

the quark mass ratio  $r$  and of the pseudoscalar masses:

$$\begin{aligned}\hat{m}B_0 &= \frac{M_\pi^2}{2(r^2 - 1)} [(r - r_1)(r + r_1 + 2) - 2\zeta(r_2 - r)(2 + r)] , \\ \hat{m}^2 A_0 &= \frac{M_\pi^2}{2(r^2 - 1)} (r_2 - r) ,\end{aligned}$$

from which one infers the expressions (18) for  $\alpha_{\pi\pi}^{lead}$  and for  $\alpha_{\pi K}^{lead}$ .

## References

- [1] H. Marsiske et al., Phys. Rev. **D41** (1990) 3324.
- [2] R. L. Goble, R. Rosenfeld and J. L. Rosner, Phys. Rev. **D39** (1989) 3264.
- [3] D. Morgan and M. R. Pennington, Phys. Lett. **B272** (1991) 134; M. R. Pennington, in *The DaΦne Handbook*, ed. by L. Maiani, G. Pancheri and N. Paver (INFN, Frascati, 1992), p.379.
- [4] J. F. Donoghue and B. R. Holstein, Phys. Rev. **D48** (1993) 137.
- [5] A. Dobado and J. R. Pelaez, Z. Phys. **C57** (1993) 501.
- [6] T. N. Truong, Phys. Lett. **B313** (1993) 221.
- [7] A. E. Kaloshin and V. V. Serebryakov, Irkutsk preprint ISU-IAP.Th 93-03 (hep-ph/93066224).
- [8] J. Gasser and H. Leutwyler, Ann. Phys. **158** (1984) 142; Nucl. Phys. **B250** (1985) 465.
- [9] J. Bijnens and F. Cornet, Nucl. Phys. **B296** (1988) 557.
- [10] J. F. Donoghue, B. R. Holstein and Y. C. Lin, Phys. Rev. **D37** (1988) 2423.
- [11] S. Bellucci, J. Gasser and M. E. Sainio, "Low-energy photon-photon collisions to two-loop order", preprint BUTP-93/18, LNF-93/077(P) and PSI-PR-93-17 (hep-ph/9401206).
- [12] N. H. Fuchs, H. Sazdjian and J. Stern, Phys. Lett. **B269** (1991) 183.
- [13] J. Stern, H. Sazdjian and N. H. Fuchs, Phys. Rev. **D47** (1993) 3814.
- [14] S. Weinberg, Physica **96A** (1979) 327.
- [15] J. Gasser and H. Leutwyler, Phys. Lett. **B125** (1983) 321.
- [16] H. Leutwyler, "On the foundations of chiral perturbation theory", preprint BUTP-93/24.

- [17] S. Weinberg, in *A Festschrift for I. I. Rabi*, edited by L. Motz (New York Academy of Sciences, New York, 1977), p. 185; J. Gasser and H. Leutwyler, Phys. Rep. **87** (1982) 77.
- [18] H. Leutwyler, Nucl. Phys. **B337** (1990) 108.
- [19] N. H. Fuchs, H. Sazdjian and J. Stern, Phys. Lett. **B238** (1990) 380.
- [20] F. G. Markopoulos-Kalamara and D. V. Bugg, Phys. Lett. **B318** (1993) 565.
- [21] Ll. Ametller, J. Bijnens, A. Bramon and F. Cornet, Phys. Lett. **B276** (1992) 185.
- [22] M. Knecht and J. Stern, in preparation.
- [23] M. Knecht, H. Sazdjian, J. Stern and N. H. Fuchs, Phys. Lett. **B313** (1993), 229.
- [24] S. Weinberg, Phys. Rev. Lett. **17** (1966) 616.
- [25] J. F. Donoghue and B. R. Holstein, Phys. Rev. **D46** (1992) 4076.
- [26] J. F. Donoghue and E. Golowich, "Chiral sum rules and their phenomenology", preprint UMHEP-389, 1993 (hep-ph/9307262).
- [27] *Review of Particle Properties*, Phys. Rev. **D45** (1992) 51.
- [28] B. Moussallam and J. Stern, to be published.
- [29] R. Omnès, Nuovo Cimento **8** (1958) 316.
- [30] P. Ko, Phys. Rev. **D41** (1990) 1531, Phys. Rev. **D47** (1993) 3933.
- [31] J. Gasser and U.-G. Meißner, Nucl. Phys. **B357** (1991) 90.
- [32] A. Schenk, Nucl. Phys. **B363** (1991) 97.
- [33] P. Eastabrooks and A. D. Martin, Nucl. Phys. **B79** (1974) 301.
- [34] W. Ochs, Thesis, Ludwig-Maximilian-Universität (1973).
- [35] J. Stern, N. H. Fuchs and M. Knecht, "Light quark masses from exclusive tau decays: An experimental proposal", preprint IPNO/TH 93-38 (hep-ph/9310299), to be published in the Proceedings of the Third Workshop on the  $\tau$  Charm Factory, 1-6 June 1993, Marbella, Spain.

## Figure captions

**Figure 1:** The vertices from  $\tilde{\mathcal{L}}^{(2)} + \tilde{\mathcal{L}}^{(3)}$  and from  $\tilde{\mathcal{L}}^{(5)}$  (for the last one) which enter the computation of the order  $O(p^5)$  amplitude  $H(s)$ . In the penultimate and antepenultimate graphs, the mass-shell conditions  $p_1^2 = p_2^2 = M_\pi^2$  for the outgoing  $\pi^0$  lines were used. The constants  $\alpha_{\pi\pi}$ ,  $\alpha_{\pi K}$ ,  $\beta_{\pi\pi}$ ,  $\beta_{\pi K}$ , as well as the constant  $c$  which appears in the last vertex, are defined in the text and in the Appendix.

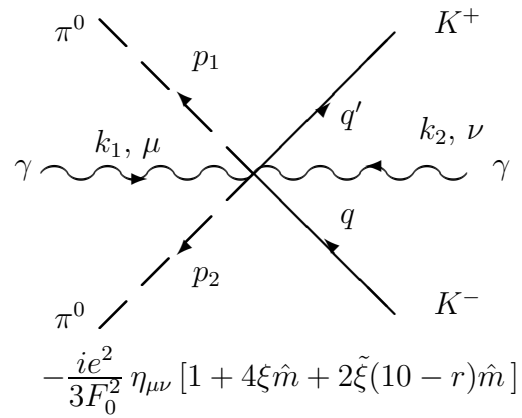
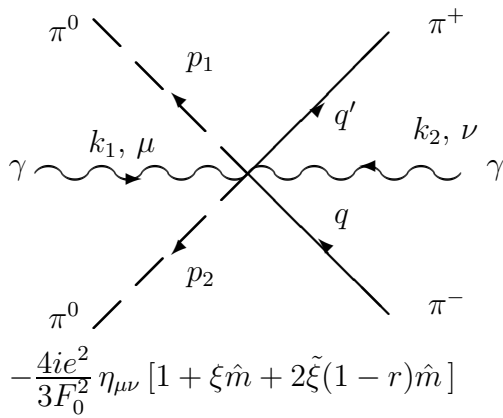
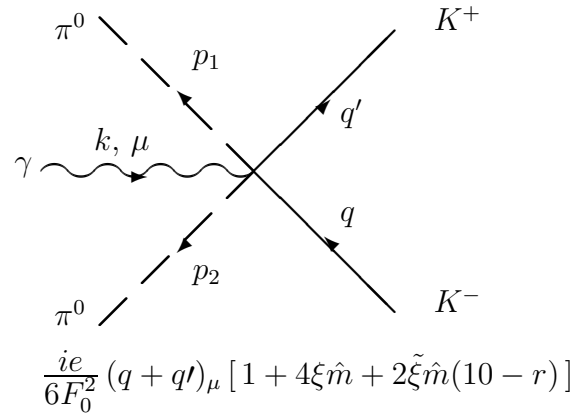
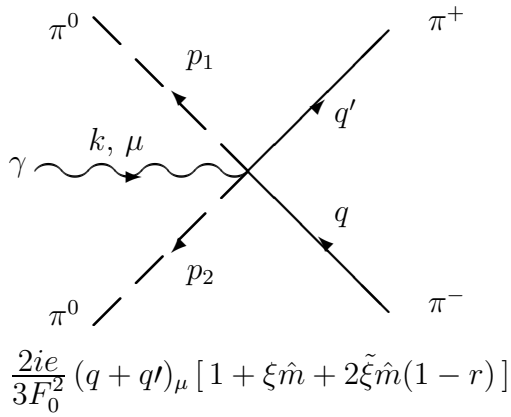
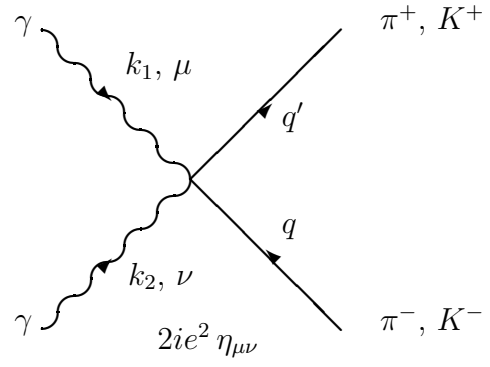
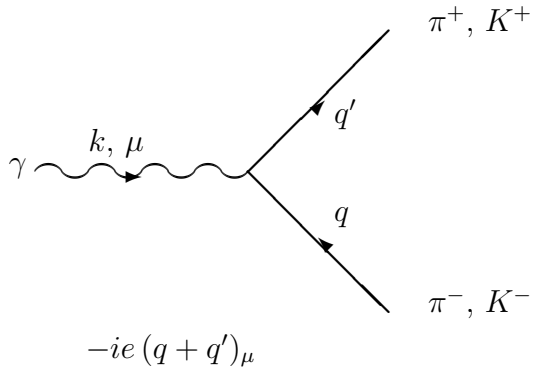
**Figure 2:** The cross section  $\sigma(\gamma\gamma \rightarrow \pi^0\pi^0, |\cos\theta| \leq Z)$  as a function of the center of mass energy  $E$  at order  $O(p^4)$  for  $r = 25.9$  (dotted line),  $r = 10$  (dash-dotted line), and for  $r = 6.3$  (solid line). The data points are taken from Ref. [1], and the vertical error bars correspond to the *statistical* errors alone.

**Figure 3:** The cross section  $\sigma(\gamma\gamma \rightarrow \pi^0\pi^0, |\cos\theta| \leq Z)$  as a function of the center of mass energy  $E$  at order  $O(p^5)$  for  $\alpha_{\pi\pi} = 1$  (dotted line),  $\alpha_{\pi\pi} = 3$  (dash-dotted line) and for  $\alpha_{\pi\pi} = 4$  (solid line), with  $\tilde{\xi}/\xi = 0$  in all three cases.

**Figure 4:** The cross section  $\sigma(\gamma\gamma \rightarrow \pi^0\pi^0, |\cos\theta| \leq Z)$  as a function of the center of mass energy  $E$  for  $\alpha_{\pi\pi} = 3$  (solid line) and the same cross section, but with  $c$  set equal to zero (dotted line). In both cases,  $\tilde{\xi}/\xi = 0$ .

**Figure 5:** The uncertainty in the order  $O(p^5)$  cross section  $\sigma(\gamma\gamma \rightarrow \pi^0\pi^0, |\cos\theta| \leq Z)$ , for  $\alpha_{\pi\pi} = 3$ , coming from the variation of the Zweig rule violating parameter  $\tilde{\xi}/\xi$  between -0.2 (lower dotted curve) and +0.2 (upper dotted curve). The solid curve corresponds to  $\tilde{\xi}/\xi = 0$ .

**Figure 6:** The order  $O(p^5)$  amplitude  $100M_\pi^2|H(s)|$ , for  $s \geq 4M_\pi^2$ , and  $100M_\pi^2H(s)$ , for  $0 \leq s \leq 4M_\pi^2$ , shown by the full line, as compared to the dispersive results obtained by matching with the  $\chi$ PT expression at  $s = 4M_\pi^2$  (dotted curve) or at  $s = 0$  (dash-dotted curve) for the set of phase shifts given by the parameters of Eq. (60) (Fig. 6a) and of Eq. (61) (Fig. 6b).



$$\begin{aligned}
& i \frac{\beta_{\pi\pi}}{F_\pi^2} (s - \frac{4}{3} M_\pi^2) + i \frac{M_\pi^2 \alpha_{\pi\pi}}{3F_\pi^2} \\
& + \frac{i}{3F_0^2} (2M_\pi^2 - q^2 - q'^2) [1 + \xi \hat{m} + 2\tilde{\xi} \hat{m} (1 - r)]
\end{aligned}$$

$$\begin{aligned}
& i \frac{\beta_{\pi K}}{4F_\pi^2} (s - \frac{2}{3} M_\pi^2 - \frac{2}{3} M_K^2) \\
& + \frac{i}{6F_\pi^2} [(M_K - M_\pi)^2 + 2M_\pi M_K \alpha_{\pi K}] \\
& + \frac{i}{12F_0^2} (2M_K^2 - q^2 - q'^2) [1 + 4\xi \hat{m} + 2\tilde{\xi} \hat{m} (10 - r)]
\end{aligned}$$

$$- \frac{4ie^2 c}{F_0^2} [k_1 \cdot k_2 \eta_{\mu\nu} - k_{1,\nu} k_{2,\mu}]$$

Fig. 1



This figure "fig1-1.png" is available in "png" format from:

<http://arxiv.org/ps/hep-ph/9402318v1>

This figure "fig1-2.png" is available in "png" format from:

<http://arxiv.org/ps/hep-ph/9402318v1>

This figure "fig1-3.png" is available in "png" format from:

<http://arxiv.org/ps/hep-ph/9402318v1>

This figure "fig1-4.png" is available in "png" format from:

<http://arxiv.org/ps/hep-ph/9402318v1>

This figure "fig1-5.png" is available in "png" format from:

<http://arxiv.org/ps/hep-ph/9402318v1>

This figure "fig1-6.png" is available in "png" format from:

<http://arxiv.org/ps/hep-ph/9402318v1>